Arabian Journal of Chemistry (2021) **14**, 103056

King Saud University

Arabian Journal of Chemistry

www.ksu.edu.sa
www.sciencedirect.com

ORIGINAL ARTICLE

Low cost and eco-friendly nanoparticles from cockle shells as a potential matrix for the immobilisation of urease enzyme

Nur Izzati Zakaria [a], Rosmawani Mohammad [a,*], Sharina Abu Hanifah [b], Khadijah Hilmun Kamarudin [c], Azrilawani Ahmad [d]

[a] *Faculty of Bioengineering and Technology, Jeli Campus, Universiti Malaysia Kelantan, 17600 Jeli, Kelantan, Malaysia*
[b] *Centre for Advanced Materials and Renewable Resources, Faculty of Science and Technology, Universiti Kebangsaan Malaysia, Bangi 43600, Selangor, Malaysia*
[c] *Advanced Nano Materials (ANoMa) Research Group, Ionic State Analysis (ISA) Laboratory, Faculty of Science and Marine Environment, Universiti Malaysia Terengganu, 21030 Kuala Nerus, Terengganu, Malaysia*
[d] *Faculty of Science and Marine Environment, Universiti Malaysia Terengganu, 21030 Kuala Nerus, Terengganu, Malaysia*

Received 5 November 2020; accepted 29 January 2021
Available online 10 February 2021

KEYWORDS

Calcium carbonate;
Cockle shell;
Enzyme immobilisation;
Nanoparticles;
Seafood waste

Abstract Cockle shells (a marine mollusc) are by-products or waste from the seafood industry, primarily made up of calcium carbonate ($CaCO_3$) and are beneficial for the immobilisation of urease (Urs). In this study, a composition of 99.5% $CaCO_3$ nanoparticles (NPs) from cockle shells was synthesised using a simple and environmentally friendly method involving the grinding and milling of cockle shells. Findings showed that the production of the pure NPs resulted in $CaCO_3$ aragonite polymorphs approximately 78 nm in size and primarily functionalised with acrylic acid N-hydroxysuccinimide ester, which had a succinimide group that bound to the amine group of Urs. Fourier Transform Infrared Spectroscopy (FTIR) spectra confirmed peaks at 1120 cm^{-1} and 1016.63 cm^{-1}, which were due to the presence of aliphatic amine C-N and amide bonds, revealing the immobilisation of Urs on functionalised NPs. Moreover, X-ray photoelectron spectroscopy (XPS) analysis showed changes in binding energy (eV) before and after immobilisation with Urs, with peaks at 131 eV and 170 eV representing phosphate and sulphur, respectively, from the Urs enzyme. Approximately 85.8% of Urs were successfully immobilised covalently on the larges

* Corresponding author.
E-mail address: rosmawani@umk.edu.my (R. Mohammad).
Peer review under responsibility of King Saud University.

Production and hosting by Elsevier

https://doi.org/10.1016/j.arabjc.2021.103056
1878-5352 © 2021 The Author(s). Published by Elsevier B.V. on behalf of King Saud University.
This is an open access article under the CC BY license (http://creativecommons.org/licenses/by/4.0/).

surface areas of the NPs, enabling greater enzyme loading for the potential development of urea biosensors.

© 2021 The Author(s). Published by Elsevier B.V. on behalf of King Saud University. This is an open access article under the CC BY license (http://creativecommons.org/licenses/by/4.0/).

1. Introduction

Cockle (*Anadara granosa*), or locally known as 'kerang' in Malaysia, is a type of bivalve shellfish that grows well in muddy coastal areas and is commonly prepared as a local dish (Mohamed et al., 2012). After consumption of cockles, the shells are left as waste and can cause foul odour due to the remaining flesh in the shells decaying or the microbial decomposition of salts into gases such as H_2S, NH_3, and amines, resulting in environmental pollution issues (Mo et al., 2018). Cockle shell waste has the potential to be re-used, which can reduce the amount of generated waste (Mo et al., 2018). The abundance of $CaCO_3$, which ranges from 95 to 99% of weight, found in cockle shells is very useful for a variety of purposes (Barros et al., 2009; Mohamed et al., 2012; Nakatani et al., 2009). The crystal structure of the raw cockle shell is made up of $CaCO_3$ aragonite, which is one of the three $CaCO_3$ polymorphs, including calcite and vaterite (Mohamed et al., 2012). Aragonite can maintain high mechanical strength and slow down the biodegradation process, thereby promoting sustained-release performance (Mailafiya et al., 2019). This makes cockle shells a potential source of $CaCO_3$ and a market for various industries such as medicines, paints, ink, paper, plastics, feedstuffs, rubbers, and adhesives (Zulkifle, 2013). In addition, nanoparticles (NPs) derived from $CaCO_3$ are biocompatible for medicine, pharmaceutical industries, and drug delivery systems (Kamba et al., 2013), and the application of other NPs and nanotechnology have also been reported in various applications (Jabir et al., 2018; Khatoon et al., 2018; Oves et al., 2018; Shaikh et al., 2017; Tabrez et al., 2020).

The size of NPs is usually between 1 and 100 nm in diameter and previous studies have shown that the physical and chemical properties of the nano-sized materials differed from bulk materials due to four factors: quantum size effect, small size effect, surface/interface effect, and macroscopic quantum tunnelling effect (Shi et al., 2014). The most important aspects in synthesising nanoparticles were the particle size, polymorphism, and morphology of the desired material, which led to the development of new materials with unique properties that differed from those of the bulk material (Kamba et al., 2013).

Different approaches, including top-down, bottom-up or combinations of both, have been used to synthesise $CaCO_3$ NPs from cockle shells. Several studies have implemented bottom-up approaches, such as the precipitation, carbonation and solution methods to synthesise $CaCO_3$ NPs. The carbonation method required very strict temperature regulations, strenuous gas bubbling phase, and utilised purified raw materials (Mailafiya et al., 2019). Although certain bottom-up methods were efficient and eco-friendly, in general, the bottom-up method was costly, complicated, and time-consuming. The addition of chemicals or surfactants can reduce the purity of the NPs because the final chemical composition of NPs would be affected (Mailafiya et al., 2019; Wang et al., 2007). Directing the reduction from the bulk was preferred by most researchers since this method allows the $CaCO_3$ in aragonite to be obtained in its natural form by retaining and protecting its unique features (Kamba et al., 2013).

Enzymes are biocatalysts that have high specificity for catalysing chemical reactions in every niche. However, the lack of long-term stability and difficulty of re-use under process conditions remains unresolved (Johnson et al., 2011). Therefore, enzyme immobilisation was one method used to ensure that the utilisation of enzymes in biotechnological processes was more favourable, practical, and cost-effective (Kausaite-Minkstimiene et al., 2011; Queiroga, 2011). The term 'immobilised enzymes' refers to enzymes that are physically or chemically confined or localised in a defined region of space while retaining catalytic activities that can be used repeatedly and continuously (Queiroga, 2011; Tamer et al., 2016). Immobilisation provides support for the enzymes and depending on the intended application, two factors, material support and immobilisation methods, have to be considered. Various methods have been utilised to immobilise enzymes, such as adsorption, covalent binding, entrapment, encapsulation, and cross-linking (Tamer et al., 2016). There have been studies on the immobilisation of urease (Urs) using nickel oxide by adsorption (Ieee et al., 2019), polypyrrole (Ppy) by entrapment (Ivanova et al., 2013), silica gel nanoparticles by cross-linking (Alqasaimeh et al., 2014), and cellulose nanomaterial by covalent binding (Wan Khalid et al., 2018). Among these methods, covalent bonding has the strongest attachment due to the formation of chemical bonds between the enzyme and the carboxyl or amine groups on the surface of a supporting matrix, which greatly reduced the leaching of the enzyme and increasing the stability (Asal et al., 2018). Furthermore, the two factors that need to be considered to obtain the most effective enzyme immobilisation are the characteristics and the nature of the support materials.

In this study, $CaCO_3$ NPs were synthesised from cockle shell waste using physical and mechanical processes without the addition of any chemicals and were then used as a matrix for the immobilisation of Urs. The surface of the NPs was primarily functionalised with acrylic acid N-hydroxysuccinimide ester to provide a succinimide group that could bind covalently to the amine group of Urs. This interaction was confirmed by Fourier Transform Infrared Spectroscopy (FTIR) and X-ray photoelectron spectroscopy (XPS) analysis.

2. Experimental methods

2.1. Chemicals

Acrylic acid N-Hydroxysuccinimide ester (NAS) was supplied by Sigma Aldrich. Phenolphthalein (PP) and the Bradford reagent were purchased from R&M Chemicals. The Urs enzyme (RN 9002-13-5; 490 units/mg from jack beans) and bovine serum albumin (BSA) with 98.0% purity were purchased from Tokyo Chemical Industry Co. and Vivantis Tech-

nologies Sdn Bhd, respectively. Phosphate-buffered solution (PBS) was prepared using di-potassium hydrogen phosphate anhydrous (K_2HPO_4) and potassium dihydrogen phosphate (KH_2PO_4) supplied by HmbG Chemicals. All chemicals were of analytical grade and used without any further purifications. All solutions and standard buffer solutions were prepared with deionised water.

2.2. Preparation of the $CaCO_3$ NPs from wasted cockle shells

The production of micro-sized particles was performed according to Islam et al. (2012) with slight modifications. Cockle shell waste obtained from seafood restaurants were cleaned and scrubbed to remove any dirt, then boiled for 10 min before being left to cool down at room temperature. Following this, the shells were washed thoroughly using distilled water and dried in an oven at 50 °C for five days before finely grounded using a blender (Seiketsu Cosmos Soylove II) and sieved using a stainless steel laboratory sieve with an aperture size of 63 μm to obtain micron-sized (10–63 μm diameter) powders.

The following procedures were carried out according to the method by Karthick et al. (2014), with some modifications, to obtain nano-sized $CaCO_3$. Micron-sized cockle shell powders were sonicated in distilled water using the QSONICA Q125 sonicator. For the sonication process, approximately 5 g of the sample was mixed in 50 mL distilled water and the total process duration was 15 min, with 3 s OFF and ON pulse simultaneously using 30% of amplitude. The products were then filtered using a filter paper and dried at 50 °C for two days in an oven.

The dry particles were milled using a planetary ball milling machine. First, a stainless steel jar (volume of 50 mL) and a stainless steel ball (diameter: 4.0 ± 0.01 mm, weight: 0.51 ± 0 .005 g/ball) were cleaned using distilled water to remove any contaminants. A quarter of the jar was filled with a 10:1 ball to sample ratio to generate a high energy impact. For milling, a rotational speed of 500 rpm was used for 3 h before the balls were removed and cleaned as the powder attached to the surface of the balls would reduce the collision energy. The same step was repeated twice with another 3 and 2 h of milling. Finally, the $CaCO_3$ NPs of cockle shells were collected and dried at 50 °C for 3 h to remove the moisture before further use.

2.3. Functionalisation of $CaCO_3$-NPs

The functionalisation of CaCO3-NPs was carried out according to a previous method (Ulianas et al., 2011). A total of 15 g NPs was suspended in 50 mL deionised water, then approximately 0.3 g of NAS was added and the mixture was stirred for 24 h at room temperature. The functionalised NPs were repeatedly washed, centrifuged, and sonicated with deionised water to reduce the pH level to pH 7. Finally, the modified NPs were dried at room temperature for 2 days and labelled as F-NPs.

2.4. Immobilisation and activity of the Urs enzyme

A combination of 94 mg NPs and 6 mg NAS was stirred in distilled water for 24 h to produce F-NPs. The F-NPs were then centrifuged and washed multiple times with PBS to remove the unbound NAS and reduce the pH level. The Urs enzyme (0.2 mL, 2.0 mg/mL of PBS) was then added to the dried F-NPs and kept at 4 °C for 24 h to allow the Urs enzyme to attach onto the surface of the F-NPs. The resulting F-NPs suspension immobilised with Urs enzyme was then centrifuged at 3000 rpm for 30 min and washed three times with 0.05 M PBS (pH 7) to remove the loosely bound Urs enzyme. The immobilised Urs was then dried and kept at 4 °C until further use.

The percentage of immobilised Urs on the surface of F-NPs was determined according to the Bradford protein assay protocol as previously described (Ulianas et al., 2011). In brief, a series of BSA concentrations ranging from 0.006 to 0.06 mg/mL were prepared to form a linear calibration graph of the BSA-protein standard. For the determination of immobilised urease adhering to the F-NPs surfaces, 100 mg F-NPs were added to 200 μL Urs (2.0 mg/mL) in a centrifuge tube and kept at 4 °C for 24 h. After 24 h, the Urs/F-NPs mixture was centrifuged and the supernatant was decanted. Following this, 60 μL of the decanted solution was then mixed with 940 μL Bradford reagent and 1000 μL deionised water then the absorbance of the solutions was measured at $\lambda = 595$ nm using the UV–Visible Spectrophotometer Cary 50. The amount of immobilised Urs was calculated according to the following equation (Alqasaimeh et al., 2014; Ulianas et al., 2011):

$$\%\text{Urs immobilised} = [(A - B)/A] \times 100\%$$

where A is the amount of Urs used and B is the concentration of the Urs left after immobilisation.

2.5. Sample characterisation

The prepared NPs were identified using FTIR in the range of 400–4000 cm^{-1} and Energy Dispersive X-Ray Analyser (EDX). The morphology and structure of the samples were analysed using a Field-Emission Scanning Electron Microscopy (FESEM, ZEISS). After the sonication and milling processes, the sizes of the NPs produced were analysed using the Particle Size Analyser (PSA, Malvern Instruments). The chemical bonds between NPs, NAS, and the Urs enzyme were determined using FTIR and XPS (Shimadzu).

3. Result and discussion

3.1. Particle size of $CaCO_3$-NPs

Table 1 shows the particle size distribution of cockle shell powders which was determined by several processes including grinding, sieving, sonication, and milling. The cockle shells were grounded and sieved using an aperture size of 63 μm siever and the sieved powders with sizes from 10 to 63 μm underwent a sonication process to reduce the particle size. However,

Table 1 The particle size distribution of cockle shell powders after the grinding, sieving, sonication and milling processes.

Process	Duration (h)	Size
After grinding and sieving	–	< 63 μm
After sonication	0.25	0.62–1.99 μm
After milling	8	68.06–91.28 nm

a long sonication period can cause agglomeration of the particles (Franco et al., 2004). In this study, a 15 min of sonication process reduced the size of the powders to within the range of 0.62–1.99 μm, thereby reducing the duration of the milling process. The average size (hydrodynamic diameter) of $CaCO_3$-NPs as measured by the PSA was 78.8 ± 10.8 nm after 8 h of milling. The particle size distribution of NPs is shown in Fig. 1.

3.2. EDX analysis of NPs

The elemental compositions of the NPs from the cockle shells were analysed by single point EDX mapping, revealing each element that was present in the sample as shown in Fig. 2. Findings showed that the NPs contained 51.3% oxygen, 30.2% calcium, 18.0% carbon, and 0.5% sodium, and had greater proportions of carbon and oxygen compared to the ratio of calcium as shown in Fig. 2. The two peaks at 2 keV and 4 keV were due to the iridium that was used to coat the surface of the NPs to prevent charging of the sample surface. This analysis has shown that the composition of NPs from cockle shells was approximately 99.5% of $CaCO_3$.

3.3. Morphological characteristics of NPs, F-NPs, and F-NPs immobilised with Urs

The morphological characteristics obtained using FESEM revealed the structure of aragonite $CaCO_3$-NPs, which were smooth and irregular in shape, as shown in Fig. 3 (a). A comparison of the images of F-NPs and F-NPs immobilised with Urs displayed in Fig. 3 (b) and (c) confirmed that F-NPs were successfully immobilised with Urs. While F-NPs (Fig. 3 (b)) typically have a smooth surface morphology, the surface structure of F-NPs changed and appeared sticky, as shown in Fig. 3 (c), after immobilisation with Urs. This indicated that the enzyme immobilisation process did not significantly agglomerate the particles and alter the structure of F-NPs. Furthermore, this also indicated that the reaction occurred only on the surface of the F-NPs through interactions between the succinimide group of NAS and the amino groups of Urs (Migliorini et al., 2018).

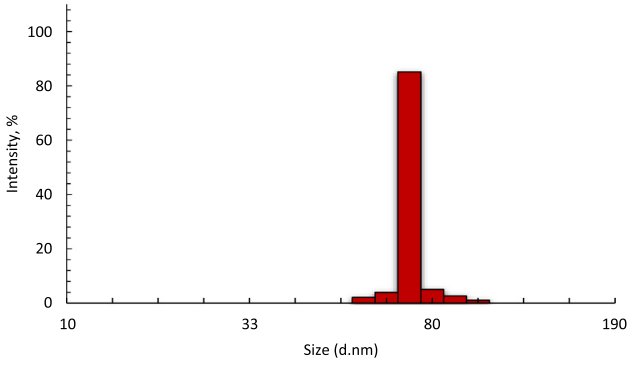

Fig. 1 The particle size distribution of NPs after 8 h of the milling process.

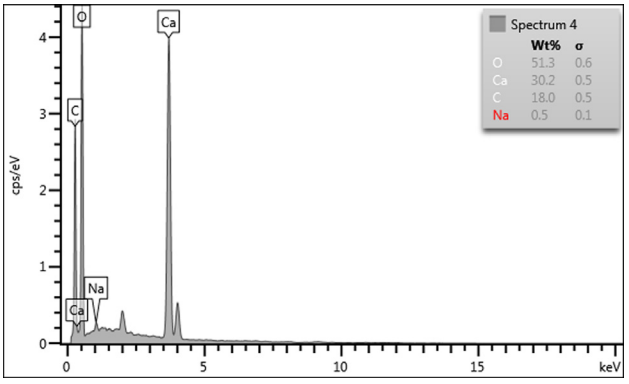

Fig. 2 Spectral peak data of $CaCO_3$ NPs from EDX spectroscopy.

3.4. FTIR analysis

In Fig. 4, the absorption peaks at 1780.74 cm^{-1}, 1444.34 cm^{-1}, 1080.93 cm^{-1}, 857.29 cm^{-1}, and 711.92 cm^{-1} from the spectral data of NPs were common characteristic features for CO_3^{2-} in $CaCO_3$ of cockle shells, as previously reported (Islam et al., 2012). The characteristic peaks representing CO_3^{2-} of aragonite were observed at 1080.93 cm^{-1} and 857.29 cm^{-1}, due to the symmetrical stretching and out-of-plane bending modes of the structure (Kamba et al., 2013). Following the addition of NAS to $CaCO_3$-NPs, the characteristic absorption of N-H stretching vibration appeared at 3368.38 cm^{-1} and peaked at 1646.55 cm^{-1} (corresponding to N-H stretching in amide II). The increased characteristic peak at 1435.96 cm^{-1} confirmed the formation of C-O bonds between $CaCO_3$ and the acrylic of NAS. Data from the FTIR spectrum after immobilisation of Urs over F-NPs showed additional bands at 1120 cm^{-1} and 1016.63 cm^{-1} due to the presence of C-N of the aliphatic amine and the amide bond, revealing the immobilisation of Urs to F-NPs (Souza et al., 2013).

3.5. XPS analysis

Analysis of two samples, one before and one after immobilisation of Urs, was performed using XPS to measure the presence of the enzyme on the functionalised $CaCO_3$. As seen in Fig. 5 (a), additional peaks were identified between 100 and 200 eV, which indicated the presence of S and P elements. The immobilisation of Urs was confirmed by the presence of sulphur through XPS analysis at around 170 eV after immobilisation, as all enzymes contain amino acids with sulphur bonds (Adeloju et al., 1993). In addition, the P peak at 131 eV demonstrated the presence of phosphate groups from the active sites of jack bean Urs, and there was no peak before immobilisation (Balasubramanian & Ponnuraj, 2010). Based on Fig. 5 (b), a peak at 284.3 eV in the spectrum after the immobilisation of Urs indicated the presence of C—C bonds, while the peak at 287 eV was related to C—O bonds, and the last peak at 287.6 eV was related to amide (C═O) bonds (Barreca & Gentile, 2018; Kahoush, 2019). The relative carbon content on the surface decreased with increased oxygen due to oxidation following Urs immobilisation (Kahoush, 2019). The increase in oxygen atoms (529 eV) and nitrogen atoms (around 400 eV) in Fig. 5 (c) and (d) after Urs immobilisation on the surface of functionalised NPs was due to increased C═O and C—N bonds respectively. Fig. 5 (d) displays a typical Ca 2p high-resolution XPS spectrum for both before and after

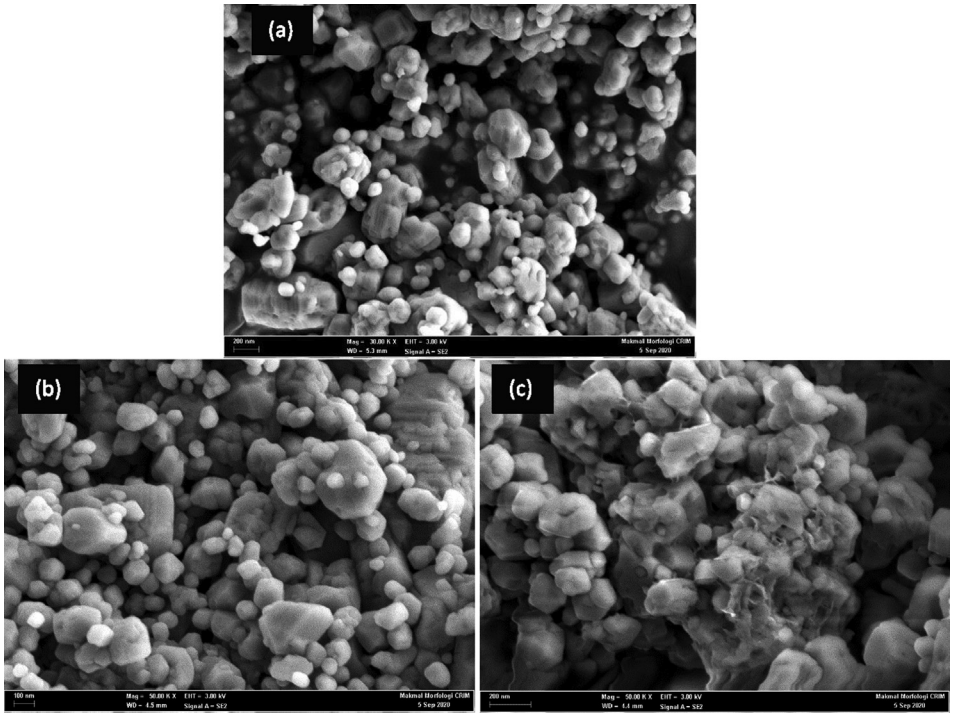

Fig. 3 FESEM images of (a) NPs, (b) F-NPs, (c) Urs/F-NPs.

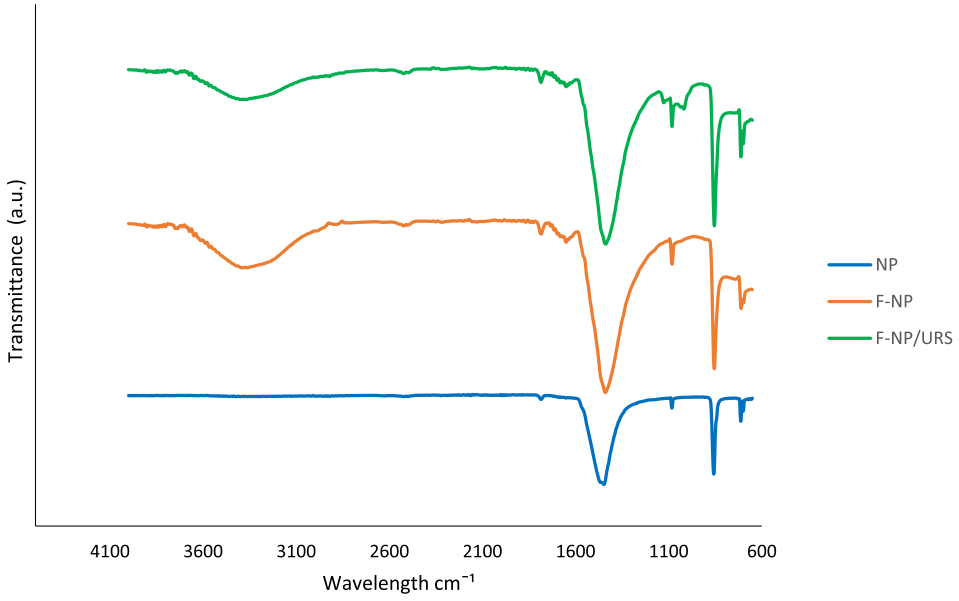

Fig. 4 FTIR spectra of the NPs, F-NPs, and Urs/F-NPs.

the immobilisation of Urs on the surface of the NPs corresponding to Ca (II) ions. The immobilisation of Urs resulted in a Ca 2p peak shift to lower binding energy, indicating interactions between functionalised NPs and Urs (Migliorini et al., 2018).

3.6. Percentage of Urs immobilised onto the matrix

The amount and percentage of Urs enzyme were quantitatively determined based on the calibration graph of standard BSA in the range of 0.006–0.06 mg/mL with $R^2 = 0.9943$, as seen in Fig. 6. The amount of Urs immobilised on different amounts of F-NPs, as calculated in Section 2.4, is shown in Fig. 7. The weight of F-NPs as a matrix affected the amount of enzyme immobilised on the F-NPs. Increased matrix weight, which provided a higher succinimide ester group, resulted in an increased amount of immobilised enzyme, demonstrating that the binding of F-NPs with Urs occurred through covalent bonding which was supported by FTIR and XPS analysis.

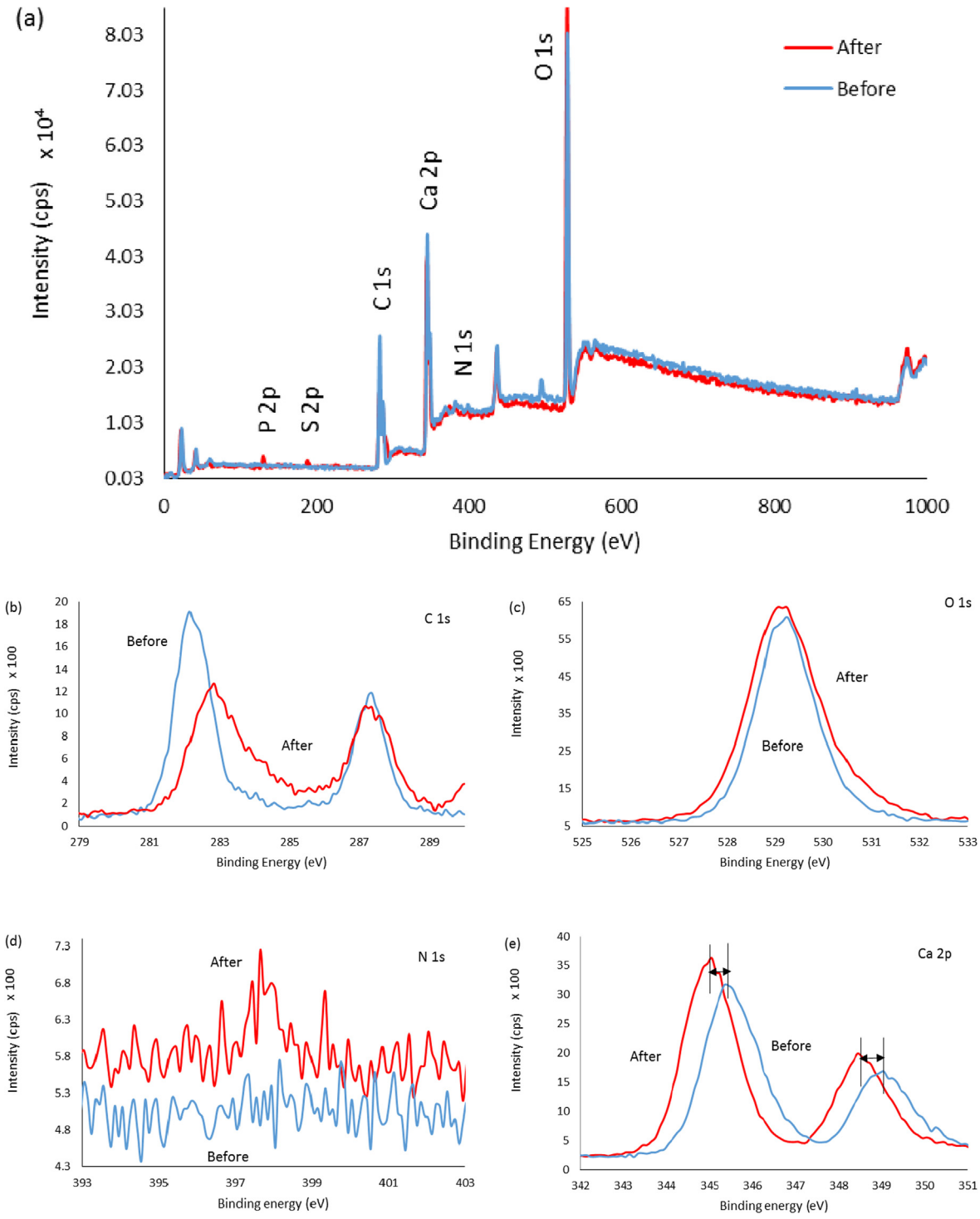

Fig. 5 A comparison of XPS spectra of F-NPs before and after immobilisation with Urs. (a) XPS survey spectra, (b) C 1s scan, (c) O 1s scan, (d) N 1s scan, and (e) Ca 2p scan.

4. Conclusions

The present study demonstrated the synthesis of $CaCO_3$ NPs using a simple and environmentally safe method from naturally available cockle shell waste for enzyme immobilisation. Both the obtained NPs and immobilised Urs were characterised using PSA, EDX, FESEM, FTIR and XPS analysis, and the NPs were identified as aragonite polymorphs of $CaCO_3$ components that were approximately 78 nm in size. The results showed a good size distribution and high purity materials. In addition, the Bradford protein assay revealed that approximately 85.8% of the Urs enzyme was successfully

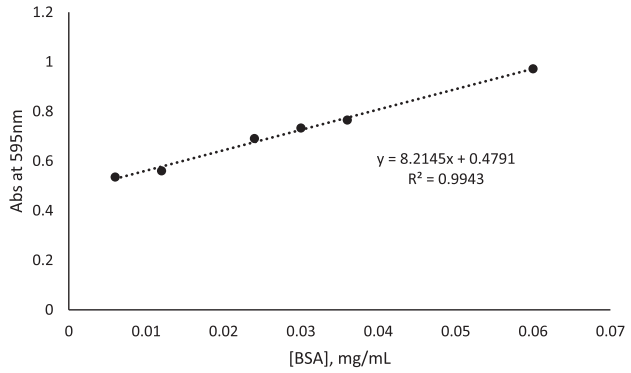

Fig. 6 Calibration graph of standard BSA.

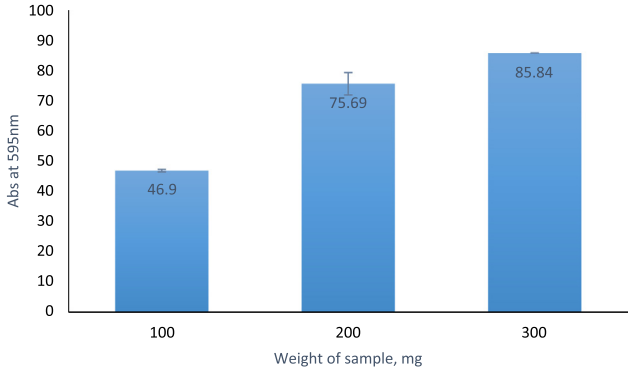

Fig. 7 The amount of Urs immobilised on the F-NPs at various sample weights.

immobilised on the F-NPs through covalent binding, giving it a high potential for urea biosensor development. Urea biosensors have the potential to be used for monitoring urea levels in human serum and urine for patients with kidney disease.

Declaration of Competing Interest

The authors declare that they have no known competing financial interests or personal relationships that could have appeared to influence the work reported in this paper.

Acknowledgements

This study was supported by the Fundamental Research Grant Scheme (FRGS), R/FRGS/A1300/01095A/003/2018/00550 from the Ministry of Higher Education.

References

Adeloju, S.B., Shaw, S.J., Wallace, G.G., 1993. Polypyrrole-based potentiometric biosensor for urea part 1. Incorporation of urease. Anal. Chim. Acta 281 (3), 611–620.

Alqasaimeh, M., Heng, L.Y., Ahmad, M., Santhana Raj, A.S., Ling, T.L., 2014. A large response range reflectometric urea biosensor made from silica-gel nanoparticles. Sensors 14 (7), 13186–13209.

Asal, M., Özen, Ö., Şahinler, M., Baysal, H.T., Polatoğlu, İ., 2018. An overview of biomolecules, immobilization methods and support materials of biosensors. Sens. Rev.

Balasubramanian, A., Ponnuraj, K., 2010. Crystal structure of the first plant urease from jack bean : 83 years of journey from its first crystal to molecular structure. J. Mol. Biol. 400 (3), 274–283.

Barreca, D., Gentile, D., 2018. Biomaterials Science graphene : effect on the activity , immobilization efficiency, and tetramer stability, 3231–3240. https://doi.org/10.1039/c8bm00850g.

Barros, M.C., Bello, P.M., Bao, M., Torrado, J.J., 2009. From waste to commodity: transforming shells into high purity calcium carbonate. J. Clean. Prod. 17 (3), 400–407.

Franco, F., Pérez-Maqueda, L.A., Pérez-Rodríguez, J.L., 2004. The effect of ultrasound on the particle size and structural disorder of a well-ordered kaolinite. J. Colloid Interface Sci. 274 (1), 107–117. https://doi.org/10.1016/j.jcis.2003.12.003.

Ieee, J.C., Member, S., Wu, C., Member, P.K.I., Member, C.L.I., 2019. The flexible urea biosensor using magnetic nanoparticles. IEEE Trans. Nanotechnol. PP(c), 1. https://doi.org/10.1109/TNANO.2019.2895137.

Islam, K.N., Zuki, A.B.Z., Ali, M.E., Bin Hussein, M.Z., Noordin, M. M., Loqman, M.Y., Abd Hamid, S.B., 2012. Facile Synthesis of calcium carbonate nanoparticles from cockle shells. J. Nanomater. 2012 (1), 1–5.

Ivanova, S., Ivanov, Y., Godjevargova, T., 2013. Urea amperometric biosensors based on nanostructured polypyrrole and poly ortho-phenylenediamine. Open J. Appl. Biosensor 02 (01), 12–19.

Jabir, N.R., Anwar, K., Firoz, C.K., Oves, M., Kamal, M.A., Tabrez, S., 2018. An overview on the current status of cancer nanomedicines. Curr. Med. Res. Opin. 34 (5), 911–921.

Johnson, P.A., Park, H.J., Driscoll, A.J., 2011. Chapter 15, 679(1), 183–191. https://doi.org/10.1007/978-1-60761-895-9.

Kahoush, M., 2019. Eco-Technologies for Immobilizing Redox Enzymes on Conductive Textiles , for Sustainable Development Doctoral dissertation.

Kamba, A.S., Ismail, M., Ibrahim, T.A.T., Zakaria, Z.A.B., 2013. Synthesis and characterisation of calcium carbonate aragonite nanocrystals from cockle shell powder (*Anadara granosa*). J. Nanomater. 2013, 1–9. https://doi.org/10.1155/2013/398357.

Karthick, R., Sirisha, P., Sankar, M.R., 2014. Mechanical and tribological properties of PMMA-sea shell based biocomposite for dental application. Procedia Mater. Sci. 6 (Icmpc), 1989–2000. https://doi.org/10.1016/j.mspro.2014.07.234.

Kausaite-Minkstimiene, A., Mazeiko, V., Ramanaviciene, A., Ramanavicius, A., 2011. Evaluation of amperometric glucose biosensors based on glucose oxidase encapsulated within enzymatically synthesized polyaniline and polypyrrole. Sens. Actuators B Chem. 158 (1), 278–285.

Khatoon, A., Khan, F., Ahmad, N., Shaikh, S., Rizvi, S.M.D., Shakil, S., Al-Qahtani, M.H., Abuzenadah, A.M., Tabrez, S., Ahmed, A. B.F., Alafnan, A., Islam, H., Iqbal, D., Dutta, R., 2018. Silver nanoparticles from leaf extract of Mentha piperita: eco-friendly synthesis and effect on acetylcholinesterase activity. Life Sciences 209, 430–434.

Mailafiya, M.M., Abubakar, K., Danmaigoro, A., Chiroma, S.M., Bin, E., Rahim, A., Moklas, M., 2019. Cockle shell-derived calcium carbonate (aragonite) nanoparticles: a dynamite to nanomedicine. Appl. Sci. 9 (14), 1–25.

Migliorini, F.L., Sanfelice, R.C., Mercante, L.A., Andre, R.S., Mattoso, L.H.C., Correa, D.S., 2018. Urea impedimetric biosensing using electrospun nanofibers modified with zinc oxide nanoparticles. Appl. Surf. Sci. 443, 18–23.

Mo, K.H., Alengaram, U.J., Jumaat, M.Z., Lee, S.C., Goh, W.I., Yuen, C.W., 2018. Recycling of seashell waste in concrete: a review. Constr Build Mater. 162, 751–764.

Mohamed, M., Yousuf, S., Maitra, S., 2012. Decomposition study of calcium carbonate in cockle shell. J. Eng. Sci. Technol. 7 (1), 1–10.

Nakatani, N., Takamori, H., Takeda, K., Sakugawa, H., 2009. Transesterification of soybean oil using combusted oyster shell waste as a catalyst. Bioresour. Technol. 100 (3), 1510–1513.

Oves, M., Aslam, M., Rauf, M.A., Qayyum, S., Qari, H.A., Khan, M. S., Alam, M.Z., Tabrez, S., Pugazhendhi, A., Ismail, I.M.I., 2018. Antimicrobial and anticancer activities of silver nanoparticles synthesized from the root hair extract of Phoenix dactylifera. Mater. Sci. Eng.: C 89, 429–443.

Queiroga, A.C., 2011. Application of immobilized enzyme technologies for the textile industry : A Application of immobilized enzyme technologies for the textile industry : a review, (November). https://doi.org/10.3109/10242422.2011.635301.

Shi, X., Gu, W., Li, B., Chen, N., Zhao, K., Xian, Y., 2014. Enzymatic biosensors based on the use of metal oxide nanoparticles. Microchim. Acta 181 (1–2), 1–22.

Shaikh, S., Rizvi, S.M.D., Shakil, S., Hussain, T., Alshammari, T.M., Ahmad, W., Tabrez, S., Al-Qahtani, M.H., Abuzenadah, A.M., 2017. Synthesis and characterization of cefotaxime conjugated gold nanoparticles and their use to target drug-resistant ctx-m-producing bacterial pathogens. J. Cell. Biochem. 9999, 1–7.

Souza, S.F.D., Kumar, J., Jha, S.K., Kubal, B.S., 2013. Immobilization of the urease on eggshell membrane and its application in biosensor. Mater. Sci. Eng. C 33 (2), 850–854.

Tabrez, S., Jabir, N.R., Adhami, V.M., Khan, M.I., Moulay, M., Kamal, M.A., Mukhtar, H., 2020. Nanoencapsulated dietary polyphenols for cancer prevention and treatment: successes and challenges. Nanomedicine 15 (11). https://doi.org/10.2217/nnm-2019-0398.

Tamer, T., Omer, A., Hassan, M., 2016. Methods of Enzyme Immobilization. Int. J. Curr. Pharm. Rev. Res. 7, 385–392.

Ulianas, A., Heng, L.Y., Ahmad, M., 2011. A biosensor for urea from succinimide-modified acrylic microspheres based on reflectance transduction. Sensors 11 (9), 8323–8338.

Wan Khalid, W.E.F., Lee, Y.H., Mat Arip, M.N., 2018. Surface modification of cellulose nanomaterial for urea biosensor application. Sains Malays. 47 (5), 941–949.

Wang, C., Liu, Y., Bala, H., Pan, Y., Zhao, J., Zhao, X., Wang, Z., 2007. Facile preparation of CaCO3 nanoparticles with self-dispersing properties in the presence of dodecyl dimethyl betaine. Colloid Surface A 297 (1–3), 179–182.

Zulkifle, A.H.B., 2013. Decomposition of Calcium Carbonate In Cockle Shell, Bachelor dissertation (May). http://umpir.ump.edu.my/.